RADIOLOGIC AND PATHOLOGIC ANALYSIS OF SOLITARY BONE LESIONS

Part III: Matrix Patterns

DONALD E. SWEET, M.D.

Chairman and Registrar, Department of Orthopedic Pathology, Armed Forces Institute of Pathology, Washington, D.C.; Clinical Associate Professor of Pathology, Uniformed Services University of the Health Sciences, Bethesda, Maryland

JOHN E. MADEWELL, M.D.

Chairman and Registrar, Department of Radiologic Pathology, Armed Forces Institute of Pathology, Washington, D.C.; Professor of Radiology and Nuclear Medicine, Uniformed Services University of the Health Sciences, Bethesda, Maryland

BRUCE D. RAGSDALE, M.D.

Staff Pathologist, Department of Orthopedic Pathology, Armed Forces Institute of Pathology, Washington, D.C.; Clinical Assistant Professor of Pathology, Uniformed Services University of the Health Sciences, Bethesda, Maryland

The preceding articles of this three-part series on radiologic and pathologic analysis of bone lesions have discussed the interface between tumor and normal bone (Part I) and periosteal responses (Part II), as well as their importance in predicting the biologic behavior of bone neoplasms. Reference was also made to the importance of location as an aid to diagnosis (Part I, Fig. 1). This segment will focus on the radiographic patterns of increased density (Fig. 1) and their significance in predicting bone tumor matrices.[18, 19] Since matrices are an important consideration in rendering specific diagnoses, a few preliminary general comments on bone tumor nomenclature are warranted.

NOMENCLATURE

Bone tumors and tumor-like conditions can be divided into matrix- and nonmatrix-producing lesions, or combinations thereof. A "matrix" refers to the acellular, intercellular substance produced by mesenchymal cells and includes osteoid, chondroid, myxoid, and collagen fibers. The mesenchymal cells synthesizing these matrices derive their names from that activity (that is, osteoblasts, cartilage cells, fibroblasts, and so forth). Similarly, matrix-producing tumors are named for the products they produce, such as osteosarcoma, chondroma, and fibroma.

Nonmatrix-producing tumors are often la-

beled by cell type (giant cell tumor), gross characteristics (cyst), or occasionally, by eponyms (Ewing's sarcoma).

The pertinent nomenclature is further modified by significant numbers of both combined matrix- and nonmatrix-producing lesions (such as in ossifying lipoma and sclerosing reticulum cell sarcoma), and mixed matrix patterns (such as in fibrous dysplasia, osteochondroma, and chondromyxoid fibroma). Even within the primary bone sarcoma group, the complexity of mixed matrix patterns and the variability of prognosis have led to subclassification. Traditional matrix lines may be designated (as in osteosarcoma, chondrosarcoma,[25] and fibrosarcoma) and increasingly, combined terms such as fibroblastic or chondroblastic osteosarcoma,[5] rather than such earlier, popular terms as "osteogenic sarcoma,"* are being used.

The assumption that matrix-producing tumors necessarily arise from mature cells of a homologous type is unwarranted[9] and is contradicted by tumors with combination patterns. The difference between the various matrices (osteoid, chondroid, and fibrous tissue) is mainly a matter of altered proportions and spatial arrangement of similar basic elements and, to a lesser extent, of the chemical details of these elements.[8] Fracture callus and some bone sarcomas (Fig. 18) present a continuum of various combinations of matrices that simultaneously emerge from the same background of synthetically active cells. Under these circumstances, there are numerous cases in which the histologic distinction between "osteoid," "chondroid," and "fibrous tissue" becomes substantially arbitrary. For this reason, the classification of matrix-producing sarcomas (which hinges on such distinctions) commonly becomes a point of endless debate.

Guidelines established since the time of Virchow state that the names of tumors should be based on the most differentiated component predominating at the site of origin. Each element of this threefold rule, to which the authors subscribe, has particular significance in the context of bone tumors. The heterogeneity of cell and matrix patterns and the variable degrees of maturation in primary bone neoplasms account for much of the difficulty associated with their interpretation. Malignant bone tumors frequently lose or significantly alter their matrix-elaborating capability once they escape the confines of bone as soft tissue extensions (Fig. 4, *D* and *E*) or metastatic foci. Diagnoses based on extramedullary material can lead to erroneous conclusions about the true nature of sarcomas of central (endosteal) origin. Similarly, sarcomas arising in association with preexisting benign lesions present complex patterns and, therefore, are special diagnostic challenges.

Frequently, two objections are raised to this threefold approach to tumor nomenclature. One has as its foundation the assumption that the tumor's name dictates a prognosis. In general, prognosis relates to the type and level of cell activity in benign lesions and to the quantity of the least differentiated elements in malignant tumors (coupled with anatomic location), rather than simply to their names. Further, and often more accurate, insight into current and potential biologic behavior can be gathered from evaluating the tumor margins and the patterns of periosteal reaction, as previously discussed in the two previous articles.

A second objection is based on the assumption that a small part of a tumor is "equivalent" to the whole. This, coupled with the urgency for treatment, invites the establishment of a diagnosis on the basis of a limited amount of biopsy material, which has often been obtained, for practical reasons, from the more readily accessible soft tissue extensions of intraosseous tumors. Even when the biopsy is obtained from the intraosseous component, it may not be entirely representative because of regional variations in histologic pattern. This discrepancy can be minimized by attention to the lesion's location (Part I, Fig. 1) in bone, because bone tumors and tumor-like lesions usually caricature normal developing bone cell patterns at the site in which they occur.[15] Of equal importance is the ability to identify the type of matrix elaborated by those tumors producing matrices through their varied radiographic mineralization patterns.[18, 19] Therefore, helpful information that may be lacking as a result of a limited amount of biopsy material is readily available in the radiographs, which reflect the bone's gross anatomy and pathology.

*The all-inclusive term "osteogenic sarcoma" was devised by early workers to avoid cumbersome, hyphenated names.[2, 3] It was applied to most malignant lesions and to some benign tumors "derived from bone and not necessarily producing bone."[6] The passage of time has not made "osteogenic sarcoma" universally specific for predominantly osteoid-producing sarcomas, and the term osteosarcoma for such tumors is preferred.[11, 12, 27, 30]

MINERALIZATION OF TUMOR MATRIX

Calcification within biologic systems generally occurs in the form of calcium hydroxyapatite. Since additional inorganic salts and a host of trace elements are usually also incorporated, "mineralization" is the preferred term. Mineralization almost invariably occurs within some form of pre-existing, substantive, organic background. Physiologic mineralization occurs in cytologically elaborated cartilage and osseous matrix. Dystrophic mineralization occurs in degenerating fibrous, myxoid, and fat tissues, whereas "metastatic" mineralization takes place in connective tissue that has been altered by metabolic disorders such as hyperparathyroidism.

Tumors may produce a matrix that is either osteoid, chondroid, fibrous (collagen), myxolipoid, or a mixture of these, but unless mineralized, it will not be visible on radiograph. The presence or absence of radiodense mineralized matrix has no bearing on the benignity or malignancy of a lesion, but its configuration may. Furthermore, a large number of lesions produce little, if any, mineralizable matrix. This discussion will be limited to the typical patterns associated with neoplastic matrices and simulated disorders, as illustrated by radiologic and pathologic correlation in selected examples.

OSSEOUS MATRIX

Bone formation is the function of osteoblastic cells. The origin of normal osteoblasts has been explained in the two preceding articles. Under normal circumstances, it occurs in the context of a pre-existent connective tissue foundation. This foundation may be: (1) collagen (intramembranous or fiber bone formation), as in the genesis of craniofacial bones and early fracture callus; (2) cartilage (enchondral bone formation), as seen at the epiphyseal and subarticular plate during growth; or (3) bone (primarily lamellar bone), as seen with internal bone remodeling.[16, 17] Three types of bone formation accounting for increased radiographic density may be associated with bone tumors and related conditions.[24] The first is direct formation of tumor osteoid or bone by neoplastic osteoblasts, as occurs in osteoblastoma and osteosarcoma. The atypical osteoid pattern of osteoid osteoma forms in a similar manner, but whether or not it is a neoplasm remains controversial.[7, 14, 23, 26] "Metaplastic tumor bone" formation as an extension of predominantly nonosseous, matrix-producing lesions occurs, for example, in fibrous dysplasia or ossifying fibroma. Similarly, "non-neoplastic," ischemic bone formation can be evoked in response to ischemically injured fat of bone infarcts and ossifying lipomas.[29] The second type of bone formation is enchondral bone formation (rings and arcs) of chondromas, and the third type is reactive new bone formation, as in reinforcing margins about benign lesions, periosteal reactions, and the sclerosing pattern that is occasionally associated with chronic inflammation. The enchondral and reactive types of bone are created by activated normal cells.

Mineralization Patterns of Tumor Bone

Mineralization of osteoid elaborated by neoplastic osteoblasts is the final step in the creation of tumor bone. When sufficient in quantity, it will be perceived in the radiograph as a homogeneous area of increased density. Degrees of density can range from a diffuse, hazy (ground glass) appearance to cloud-like and ivory-like patterns (Fig. 1).

Osteoblastomas are benign osseous tumors that predominantly occur in the axial skeleton and metaphysis of adolescent long bones and tend to grow as centrifugal masses.[13] Most osteoblastomas appear as round to oval lucent lesions on radiography (Fig. 2*A*), despite the presence of considerable tumor osteoid (Fig. 2*B*) because it is not mineralized. In those osteoblastomas in which tumor matrix tends to coalesce and subsequently to mineralize (Fig. 3*B*), the radiograph will demonstrate a well-circumscribed, central area of homogeneous cloud-like density (Fig. 3*A*). The cytologically active peripheral margin of such lesions usually remains lucent (Fig. 3*A*, *arrow*).

Osteosarcomas predominate in the metaphysis of growing long bones. They may arise within the medullary cavity (central)[14] or on the surface of bone (parosteal).[32] Most central osteosarcomas are high-grade malignant tumors; most parosteal lesions are of a lower grade. The essential histologic finding in osteosarcoma is a predominance of neoplastic osteoid formed directly by sarcoma cells. Because of considerable histologic variability, a number of subtypes have been identified.[5]

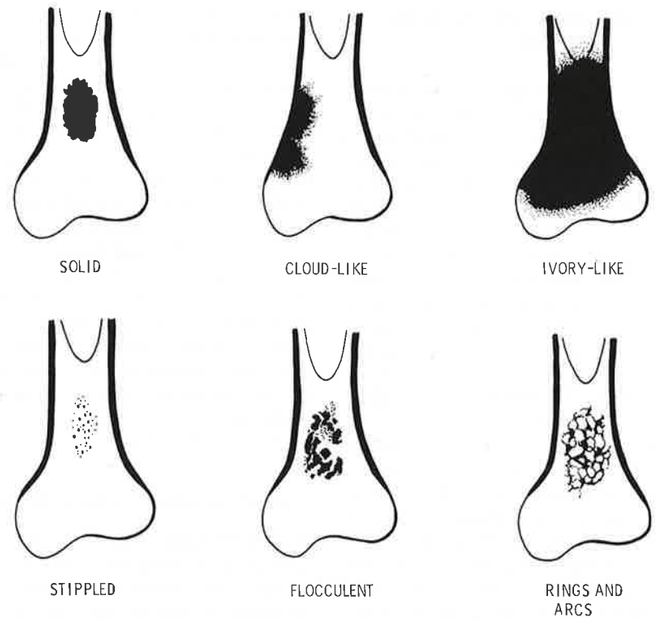

Figure 1. Schematic diagram of mineralized matrix patterns. Tumor osteoid appears as increased density with a solid (sharp-edged) or cloud to ivory-like (ill-defined edge) pattern. Tumor cartilage creates stippled, flocculent, and solid density patterns. Rings and arcs represent bony rims about tumor cartilage lobules. Dystrophic mineralization and ischemic osteoid tend to mimic the stippled, flocculent, or patchy solid density pattern.

Figure 2. Unmineralized osteoid matrix; osteoblastoma of the femur. *A* A clinical tomographic view demonstrates a small, well-circumscribed, lucent defect in the intertrochanteric area of the left femur. *B*, A photomicrograph (magnification × 63) reveals short, irregular spicules of immature, unmineralized osteoid being formed by plump osteoblastic cells. The background is highly vascular and osteoclastic giant cells are abundant. (AFIP Neg. Nos. 81-2422, 81-16750.)

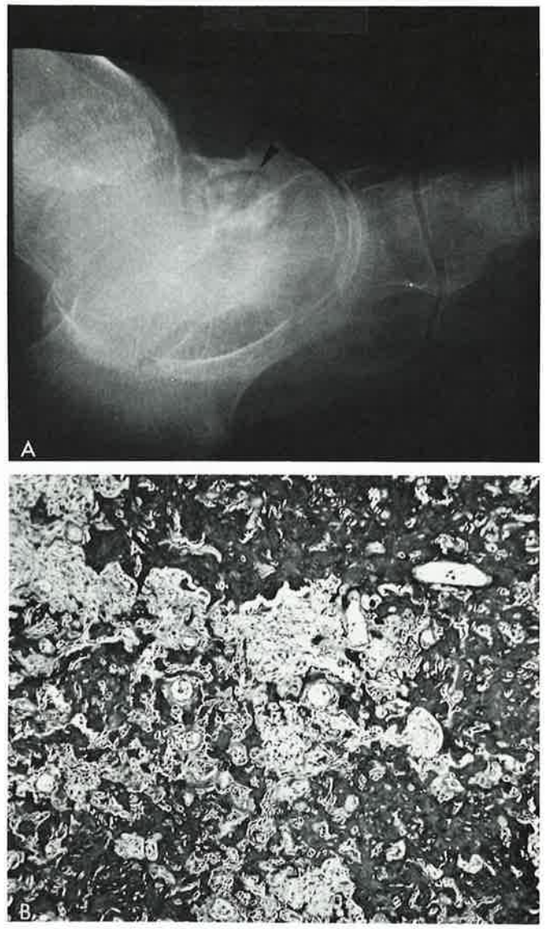

Figure 3. Cloud-like density; osteoblastoma of the talus. *A*, A clinical radiograph reveals a well-circumscribed lesion with central density and a peripheral rim of lucency (*arrow*). The cloud-like densities are patchy with fairly sharp edges. *B*, A photomicrograph (magnification × 63) reveals a coalescing pattern of atypical tumor osteoid matrix being produced by osteoblastic cells. The more deeply basophilic staining of the tumor bone denotes phosphate and correlates with mineralization. (Equating basophilia with mineralization in histologic sections is not strictly correct since the tissue is decalcified prior to sectioning. The more deeply basophilic staining of matrix denotes residual phosphate which corresponds to areas of previous mineralization.) (AFIP Neg. Nos. 77-5870-2, 81-16749.)

The bone matrix produced by osteosarcoma ranges from well-formed trabeculae of the uncommon low-grade intraosseous variant, to waxy-appearing osteoid of the sclerosing type. Pleomorphic, telangiectatic, myxoid, and fiber-rich variants are also seen. Subclassification of osteosarcoma is also based, in part, on the radiographic image created.

The radiograph of a typical osteosarcoma (Fig. 4*A*) often reveals a combination form of lytic destruction with variously sized, ill-defined, hazy to cloud-like, and even solid, ivory-like fields of increased density within the medullary cavity. The areas of increased density, whether patchy or diffuse, hazy or solid, are usually homogeneous and have ill-defined edges. They result from formation of mineralized tumor bone by the sarcoma as it infiltrates the marrow space, frequently going between intact, residual, normal bone trabeculae (Fig. 4, *C* and *D*). Once a sarcoma escapes the confines of the medullary cavity and extends beyond the cortex, it may become altered or it may even lose its matrix-producing capability (Fig. 4, *B* and *C*). Often, it will form chondroid matrix (which may or may not mineralize) or no matrix at all (Fig. 4*E*). The patchy, cloud-like pattern of density (Fig. 5*A, arrow*) may coalesce into a diffuse, ivory-like density (Fig. 5*A, curved arrow*). The range of increased density results from the varying amounts and degrees of mineralization of tumor bone matrix (Fig. 5, *B* and *C*). Radiotherapy can also quickly increase the

Text continued on page 792

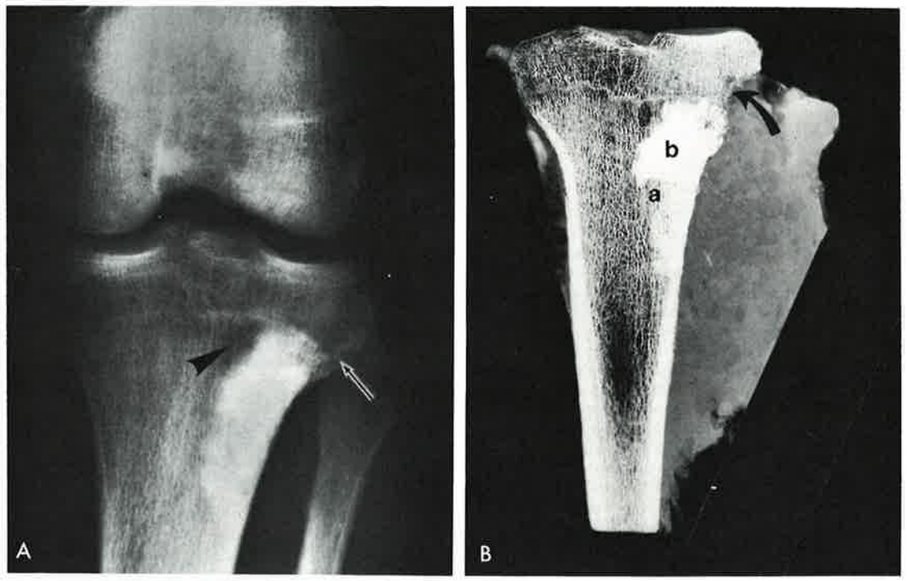

Figure 4. Cloud-like density; osteosarcoma of the tibia. *A*, A clinical radiograph demonstrates homogeneous, cloud-like, and solid patterns of increased density with ill-defined edges in the lateral metaphysis of the tibia. Regional osteoporosis about the knee, secondary to hyperemia, is to be distinguished from the focal area of lytic destruction at the superior edge of the tumor density (*arrowhead*). The only radiographic clue of the clinically palpable soft tissue mass is localized irregularity and destruction of the cortex (*arrow*). B, The specimen radiograph of the proximal end of the resected tibia demonstrates in better detail the cloud-like increased density, soft tissue extension, and cortical irregularity and destruction. Within the portion of increased density, coalescence of tumor bone and cancellous bone creates a continuum, with some areas of hazy density (a) and other areas of complete obliteration of cancellous architecture (b). The proximal focus of lytic destruction (*curved arrow*) consists of the more cellular sarcoma seen in the macrosection (see *C*, *curved arrow*).

Illustration continued on opposite page

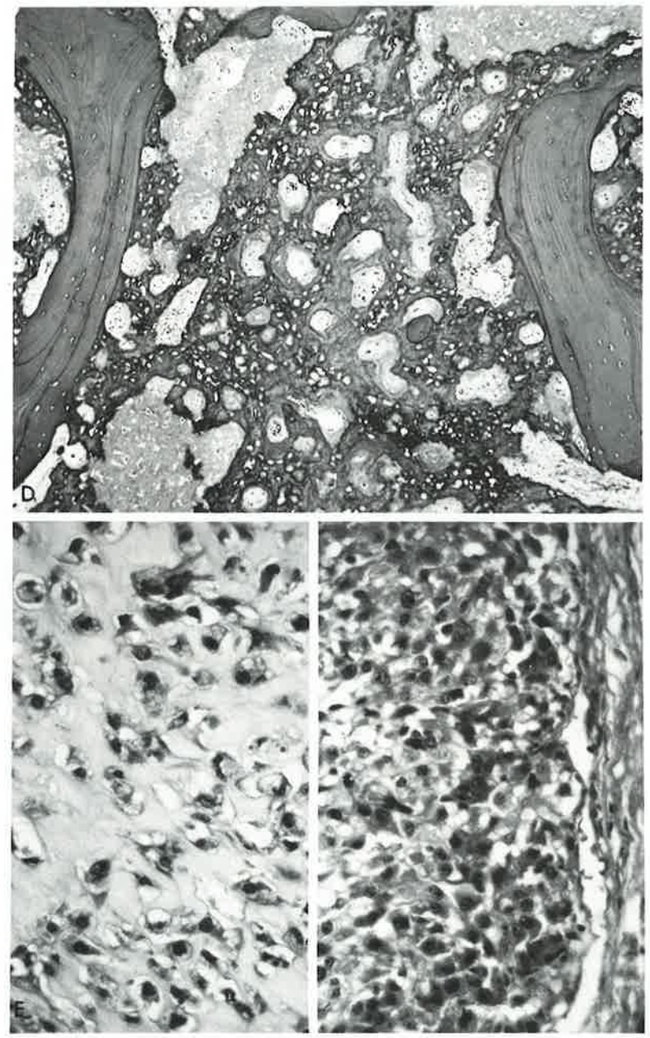

Figure 4 Continued. *C*, The macrosection corroborates the specimen radiograph (in *B*) in depicting basophilic tumor bone within the tibia. One area is deeply basophilic (b), whereas the other (a) is less basophilic, corresponding to the degree of mineralization and density seen in the radiographs (*A* and *B*). This plane of section indicates considerable cortical destruction, soft tissue extension, and evidence of vascular invasion beyond the pseudocapsule (*arrowheads*). *D*, A photomicrograph (magnification × 63) taken from the solid dense area (b in *C*) reveals tumor bone completely filling the marrow space between cancellous trabeculae. Tumor bone is also seen to be applied to the surface of the pre-existing cancellous bone trabeculae. The combination of pre-existing cancellous bone plus mineralized tumor bone creates the cloud-like to solid patterns in the clinical and specimen radiographs. *E* (*left*), A photomicrograph (magnification × 250) from the central portion of the soft tissue extension demonstrates a pattern of chondrosarcoma in which atypical chondrocytes in large lucunae are separated by the cartilage matrix. *E* (*right*), The peripheral-most proliferative zone of the soft tissue extension consists of pleomorphic malignant cells with no evidence of matrix production. This tripartite tumor illustrates the potential of a limited (especially extraosseous) biopsy to be diagnostically misleading. (AFIP Neg Nos. 79-1676, 81-14584, 81-14525, 81-14531, 81-14529.)

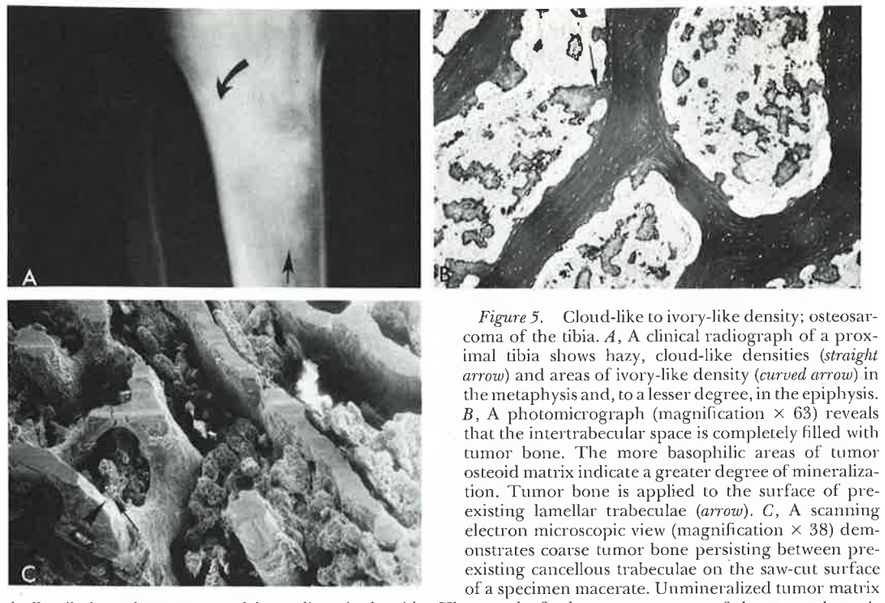

Figure 5. Cloud-like to ivory-like density; osteosarcoma of the tibia. *A*, A clinical radiograph of a proximal tibia shows hazy, cloud-like densities (*straight arrow*) and areas of ivory-like density (*curved arrow*) in the metaphysis and, to a lesser degree, in the epiphysis. *B*, A photomicrograph (magnification × 63) reveals that the intertrabecular space is completely filled with tumor bone. The more basophilic areas of tumor osteoid matrix indicate a greater degree of mineralization. Tumor bone is applied to the surface of preexisting lamellar trabeculae (*arrow*). *C*, A scanning electron microscopic view (magnification × 38) demonstrates coarse tumor bone persisting between preexisting cancellous trabeculae on the saw-cut surface of a specimen macerate. Unmineralized tumor matrix and all cells have been removed by sodium hydroxide. The rough, finely porous texture of the tumor bone is attributable to the close spacing of lacunae containing malignant osteocytes. The tumor attachment points to antecedent cancellous trabeculae (*arrow* and *arrowhead*). (AFIP Neg Nos. 81-14660, 81-14534, 81-14539.)

quantity of mineralized matrix that is radiographically apparent. The diffuse, solid, ivory-like radiographic appearance of a "sclerosing" osteosarcoma (Fig. 6*A*) is a result of the almost complete replacement of the intertrabecular marrow space by mineralized osseous tumor matrix (Fig. 6, *B* and *C*). The continuum of normal trabecular bone, together with the varying amounts of intervening mineralized tumor bone filling the marrow space, accounts for the transition from hazy to cloud-like and solid, ivory-like radiographic patterns. Occasionally, primary bone sarcomas elaborate a matrix with the combined histologic characteristics of chondroid and osteoid and these often demonstrate dense radiographic images similar to those shown in Figures 5*A* and 6*A*.

A coarsely textured, almost trabecular pattern of tumor bone tends to emerge in osteosarcomas with a fibrous or fibroblastic background, as are often encountered with low-grade parosteal osteosarcomas (Fig. 7) and the occasional central fibroblastic osteosarcoma. This pattern offers a striking contrast to the diffuse, cloudy, and homogeneous patterns previously described. The coarsely textured, spiculated radiographic appearance (Fig. 7*A*, zone c) is best appreciated in the specimen radiograph (Fig. 7*B*, zone c), and is attributable to woven tumor bone being formed within the context of a fibroblastic background. The progressive coalescence of the coarsely textured patterns with more densely sclerotic areas (Fig. 7, *A* and *B*, zone b) indicates increasing conversion of the neoplastic fibrous component to tumor bone.

Tumors arising from surface periosteum (parosteal sarcomas) tend to act in a relatively low-grade malignant fashion compared with their intraosseous counterparts. Those primary intraosseous sarcomas that mimic the histologic features of parosteal sarcoma also tend to act somewhat less aggressively[31] than the more common, high-grade osteosarcomas (see Figs. 4, 5, and 6). The diffuse, homogeneous, intraosseous pattern of density with ill-defined edges that is characterized by atypical, waxy, osteoid matrix is usually indica-

Text continued on page 796

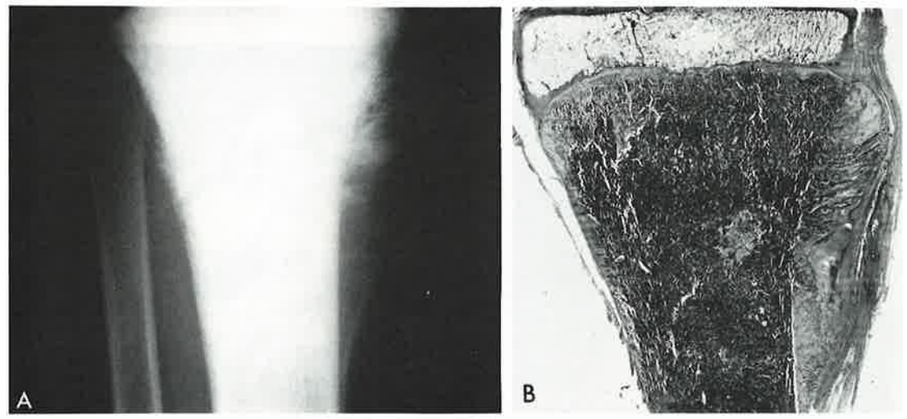

Figure 6. Ivory-like density; osteosarcoma of the sclerosing type affecting the tibia. *A*, A clinical radiograph reveals a diffuse, ivory-like, sclerosing pattern that occupies the entire metaphysis to the level of the epiphyseal growth plate. Soft tissue extensions have infiltrated a spiculated periosteal reaction, creating a "sunburst" effect. *B*, The correlating macrosection (magnification × 1) indicates that the entire metaphysis is replaced by darkly basophilic tumor osteoid between normal bone trabeculae. The epiphyseal growth plate has served as a barrier against extension of the tumor into the epiphysis. *C*, A photomicrograph magnification × 251) reveals that the intertrabecular marrow space is completely filled with tumor bone, which is more darkly stained than is the adjacent normal bone. Mineralized tumor osteoid masks the normal cancellous radiographic architecture of the metaphysis by cloaking the pre-existent trabeculae; this accounts for the homogeneous, ivory-like, increased density. (AFIP Neg. Nos. 67-11194, 81-14516, 81-14503.)

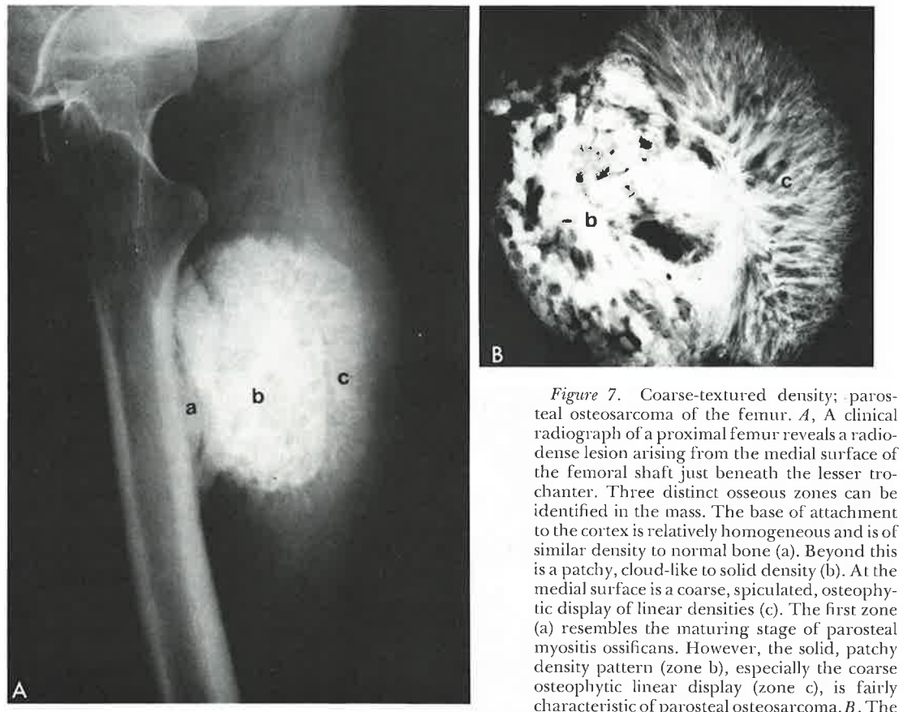

Figure 7. Coarse-textured density; parosteal osteosarcoma of the femur. *A*, A clinical radiograph of a proximal femur reveals a radiodense lesion arising from the medial surface of the femoral shaft just beneath the lesser trochanter. Three distinct osseous zones can be identified in the mass. The base of attachment to the cortex is relatively homogeneous and is of similar density to normal bone (a). Beyond this is a patchy, cloud-like to solid density (b). At the medial surface is a coarse, spiculated, osteophytic display of linear densities (c). The first zone (a) resembles the maturing stage of parosteal myositis ossificans. However, the solid, patchy density pattern (zone b), especially the coarse osteophytic linear display (zone c), is fairly characteristic of parosteal osteosarcoma. *B*, The specimen radiograph of the resected parosteal mass shows the central, patchy, cloud-like to solid density (b) and the peripheral, coarse, spiculated, osteophytic density (c) in greater detail.

Illustration continued on opposite page

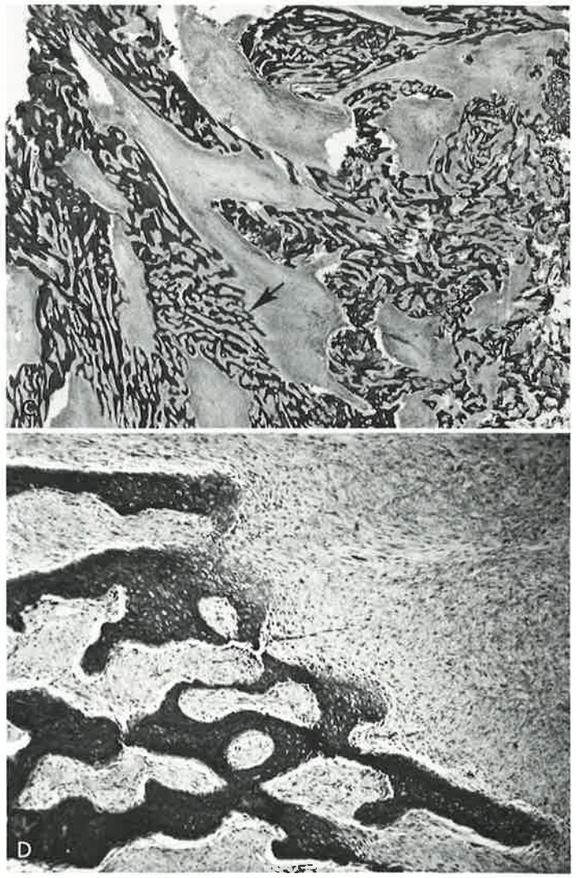

Figure 7 Continued. *C*, A photomicrograph (magnification × 10) from the osteophytic zone (*B*, zone c) shows that the spicules consist of closely packed, coarse strands of fiber bone (*arrow*). The lucent areas between the tumor bone spicules are filled with sarcomatous fibrous tissue. *D*, A photomicrograph at higher power (magnification × 63) of the edge of the tumor bone spicule (marked by the arrow in *C*) demonstrates the cellular sarcomatous bone with a woven pattern on the left and the malignant fibrous tissue from which it arises on the right. (AFIP Neg. Nos. 79-2964-1, 81-14542, 81-14509, 81-14547.)

tive of high-grade sarcoma and is in sharp contrast to the coarsely textured, cancellous-like, spiculated pattern. Thus, it may be possible to differentiate between high- and low-grade malignant, osseous, matrix-producing tumors in some cases, not only by location, destructive margins, and periosteal reactions, but also by matrix patterns reflected in the radiograph.

"Metaplastic" Patterns of Bone Mineralization

Although bone, including tumor bone, is elaborated by osteoblastic cells, it is occasionally produced through conversion of antecedent fibroblastic cells into functional osteoblasts. The production of fiber bone is easily perceived during periods of rapid, periosteal, new born formation (Part II, Figs. 11*B* and 22*I*). When this occurs in basically fibrous tumors, as is characteristically observed in fibrous dysplasia (Fig. 8, *B* and *C*), the pattern of bone formed within the space-occupying mass is also woven or fibrous in appearance (Fig. 8*C*). It is characterized by increased numbers of osteocytes, and reveals a randomly woven collagen pattern when viewed with polarized light. Woven bone of this type is usually less densely mineralized than is tumor bone that is directly formed by neoplastic osteoblasts. This relatively sparse amount of uniformly distributed, poorly mineralized, woven bone results in the hazy, ground glass, radiographic appearance of fibrous dysplasia (Fig. 8*A*). Larger amounts of fiber bone laid down on pre-existing spicules may create coalescent, patchy, cloud-like densities (Fig. 8, *A* and *B*). Only rarely is the woven bone that is formed in fibrous dysplasia sufficient to produce patchy, solid areas. This type of patchy, solid density is more likely to be seen in the more mature stages of ossifying fibroma of the craniofacial skeleton.

Ischemic injury or necrosis of marrow fat, whether in the context of bone infarct or avascular necrosis, results in the development of a reactive interface between necrotic and viable tissues.[28] Similar changes occur within intraosseous lipomas and following radiation necrosis. The presence of fat necrosis in bone typically results in the formation of dense, hyalinized, fibrous tissue. Within these foci of modulating fibrosis and nearby ischemically injured fat, both dystrophic mineralization (see separate section) and "ischemic" ossification (Figs. 9*E*, 10*C*, and 11*D*) can be identified histologically. "Ischemic" bone is usually demonstrated in the radiograph as linear or small, solid, patchy foci of increased density. In bone infarcts (Fig. 9), the density pattern is distributed within the reactive interface around the infarct's perimeter, between the dead fat and viable marrow. In ossifying lipomas (Fig. 10*A*), the density pattern is usually seen centrally as patchy, solid areas (Fig. 10, *C* and *D*) or less commonly, peripherally, as part of a reinforcing margin about a lipoma (Fig. 10*A*). With radiation-induced injury, the increased density associated with necrosis and fibrosis may be scattered throughout the irradiated area and its pattern will be less predictable (Fig. 11*A*). Histologically, it is remarkably similar to the ischemic changes noted above (Fig. 11*D*).

Enchondral Patterns of Bone Mineralization

Chondromas (enchondromas, cortical chondromas, or osteochondromas), like the physeal growth plate from which most of them originate, are capable of undergoing complete cartilage maturation, including provisional calcification and induction of enchondral bone formation. The lobular architecture of chondromas results in the formation of rings and arcs of bone (see Fig. 13). Unlike true metaplastic bone, in which the functional osteoblasts modulate from pre-existing tumor stroma, the osteoblasts forming the arcs and rings of bone in chondromas differentiate from the normal marrow reservoir. Although not really a neoplastic matrix, this pattern is distinctively chondromatous, and will be discussed in greater detail in the section on cartilage matrix.

Reactive Patterns of Bone Mineralization

Reactive bone is formed through osteoblastic modulation of normal marrow or soft tissue elements as an appliqué on pre-existing cancellous or cortical bone surfaces, or as a periosteal reaction. Reactive bone associated with bone tumors usually is manifested by reinforced margins (Part I, Fig. 3), slow periosteal reactions (Part II, Fig. 2) around slowly progressive, intraosseous lesions, or rapid periosteal reactions (Part II, Fig. 2) in response to aggressive intraosseous tumors. Occasionally, slowly progressive neoplastic lesions, such as hemangiomas, and certain malignant ones, such as reticulum cell sarcomas,

Text continued on page 802

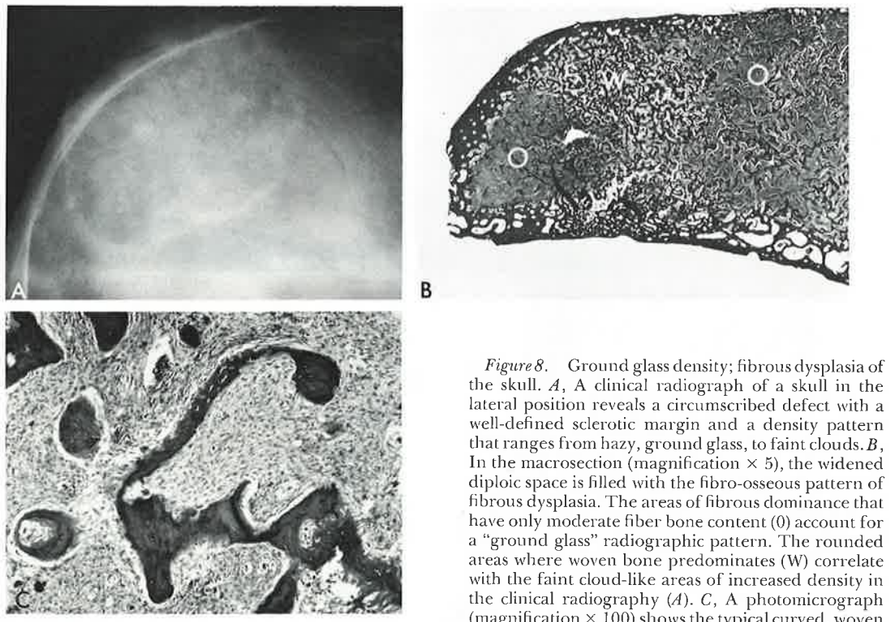

Figure 8. Ground glass density; fibrous dysplasia of the skull. *A*, A clinical radiograph of a skull in the lateral position reveals a circumscribed defect with a well-defined sclerotic margin and a density pattern that ranges from hazy, ground glass, to faint clouds. *B*, In the macrosection (magnification × 5), the widened diploic space is filled with the fibro-osseous pattern of fibrous dysplasia. The areas of fibrous dominance that have only moderate fiber bone content (0) account for a "ground glass" radiographic pattern. The rounded areas where woven bone predominates (W) correlate with the faint cloud-like areas of increased density in the clinical radiography (*A*). *C*, A photomicrograph (magnification × 100) shows the typical curved, woven bone ossicles formed by cells which have modulated from the fibrous component. The degree and distribution of this modulation dictates the radiographic pattern. (AFIP, Neg. Nos. 56-18465, 75-17058, 81-14788.)

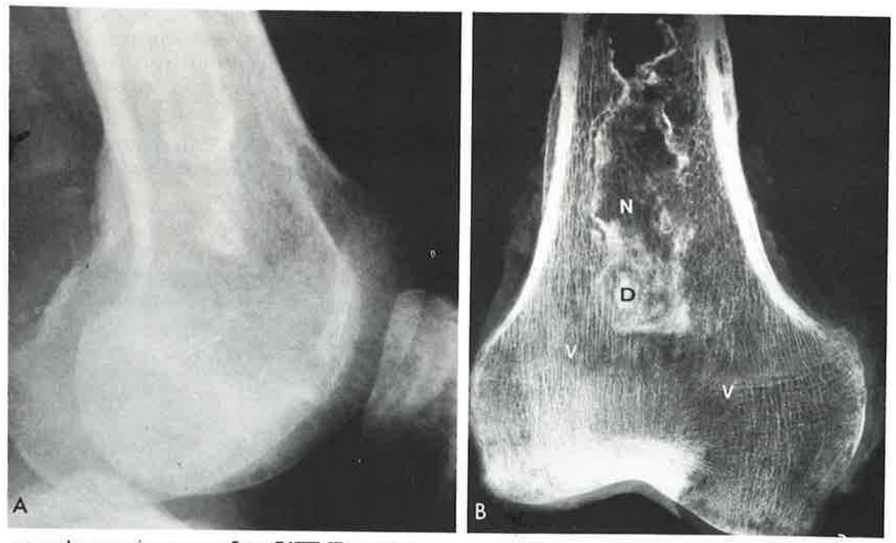

Figure 9. Stippled, flocculent, and patchy solid density; bone infarct of the femur. *A*, A lateral view of the distal femur demonstrates an irregular but discrete endosteal density. The density is concentrated at the periphery of the lesion in a combined stippled, flocculent, patchy solid, and curvilinear pattern. *B*, A specimen radiograph of a coronal section reveals unaltered density within the central necrotic zone (N). This zone is separated from the adjacent viable bone and marrow (V) by an irregular curvilinear margin of increased density. The localized area of increased density (D) that appears within the inferior portion of the infarct is an "en face" view of the mineralized margin. *C*, A macroscopic section (magnification ×2) shows the essentially unchanged central necrotic zone (N) which is separated from the adjacent, viable, endosteal cavity (V) by a narrow, more darkly stained, reactive, ischemic zone (*arrow*). The dark-stained areas are phosphate-rich as a result of mineralization, and correspond to the distal radiodense areas in the specimen photograph (Fig. *B*). The dark-staining patch (D) occurs where the plane of section has cut into the undulating reactive margin (Fig. *E*).

Illustration continued on opposite page

Figure 9 Continued. *D*, A photomicrograph (magnification × 18) of the reactive interface margin (I, *horizontal line*) which separates necrotic (N) from viable (V) bone and marrow. Note the foci of ischemic bone formation (*arrowhead*) and the dystrophic mineralization of necrotic fat (*thick arrows*). Essentially unaltered cancellous bone traverses all three zones (*thin arrows*). *E*, A photomicrograph (magnification × 18) of the inferior portion of the infarct (D in Figs. *B* and *C*) reveals a densely basophilic area which is composed of a combination of ischemic bone formation and dystrophic mineralization. The immediate fibrotic (*gray*) area around this region shows a large number of cholesterol crystals that are the result of fat breakdown. This summation of ischemic bone and dystrophic mineralization in and about the peripheral reactive interface of the infarct gives rise to the stippled, flocculent, patchy, solid, and curvilinear density patterns best appreciated in the specimen radiograph (*B*). (AFIP Neg. Nos. 65-5966-3, 79-5408, 79-15021-3, 79-15021-1,4.)

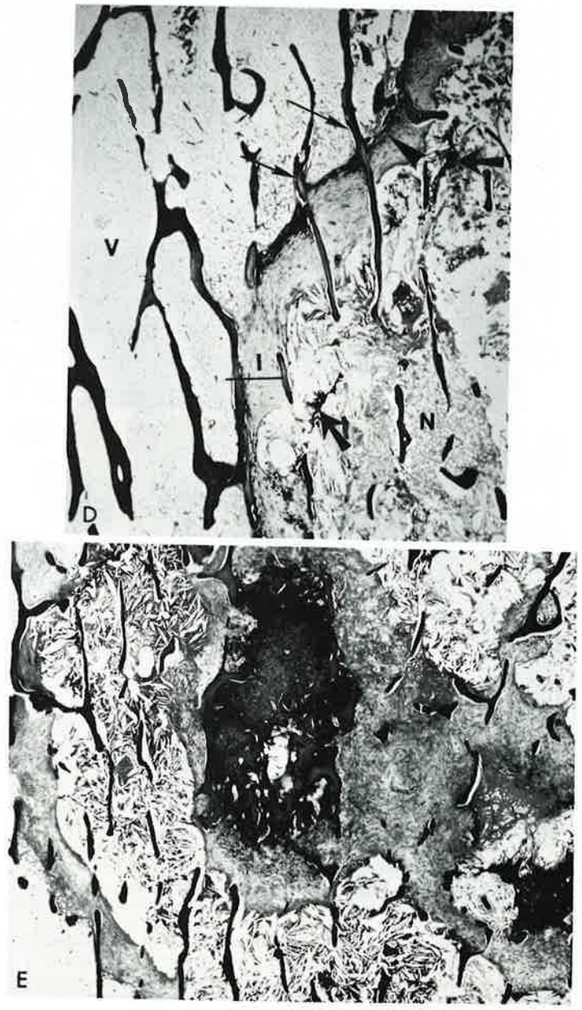

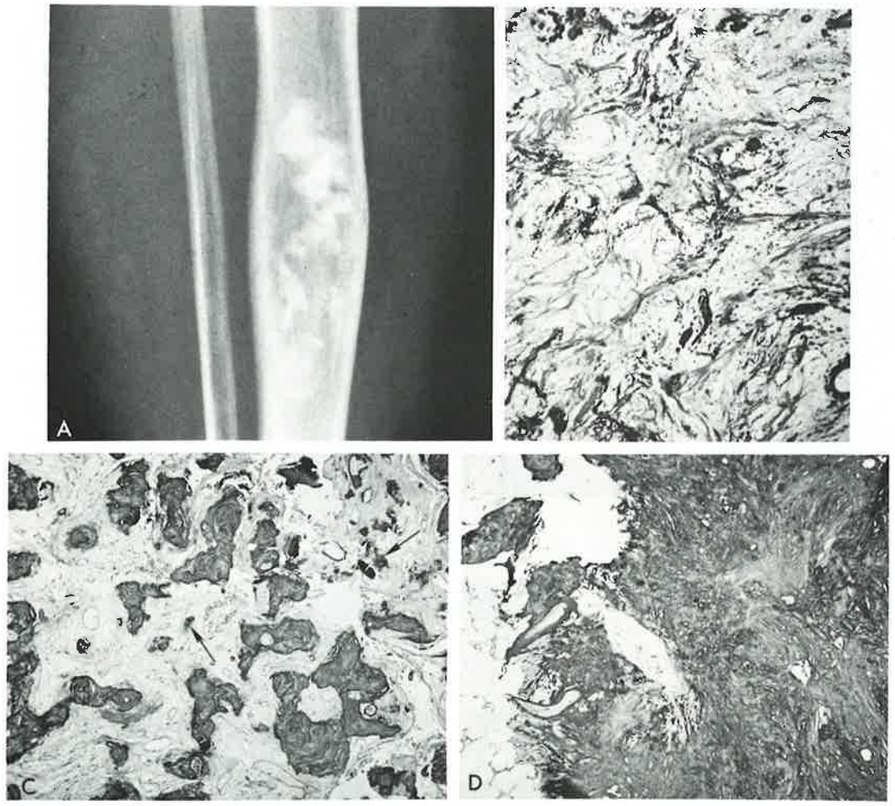

Figure 10. Solid, patchy density with some stipples and floccules; ossifying lipoma of the tibia. *A*, A clinical radiograph reveals a dominantly lucent lesion in the midshaft of a tibia with a widened bone contour. Within the lucent lesion are flocculent to patchy solid density patterns and some stipples. The sclerotic rim at the inferior margin is reminiscent of that seen with a bone infarct, but the widened bone contour excludes this and indicates a slowly enlarging, space-occupying lesion. *B*, A photomicrograph (magnification × 157) shows finely granular, dystrophic mineralization encrusting the fibrous component of the hypocellular myxolipoid substance of the lesion. *C*, Another photomicrograph (magnification × 63) demonstrates ischemic osteoid emerging from a hyalinized myxofibrous background. The dark basophilic reversal and resting lines give it a mosaic quality that superficially is reminiscent of Paget's disease. Foci of dystrophic mineralization within the hyalinized fibrous stroma are marked by arrows. *D*, Still another photomicrograph (magnification × 157) shows a pattern of coalescing dystrophic mineralization of injured fat and densely mineralized ischemic osteoid. This correlates with the patchy areas of solid density seen in the clinical radiograph (*A*). Mature fat cells are seen along the top margin. (AFIP Neg. Nos. 81-2504, 81-16755, 81-16757, 81-16756.)

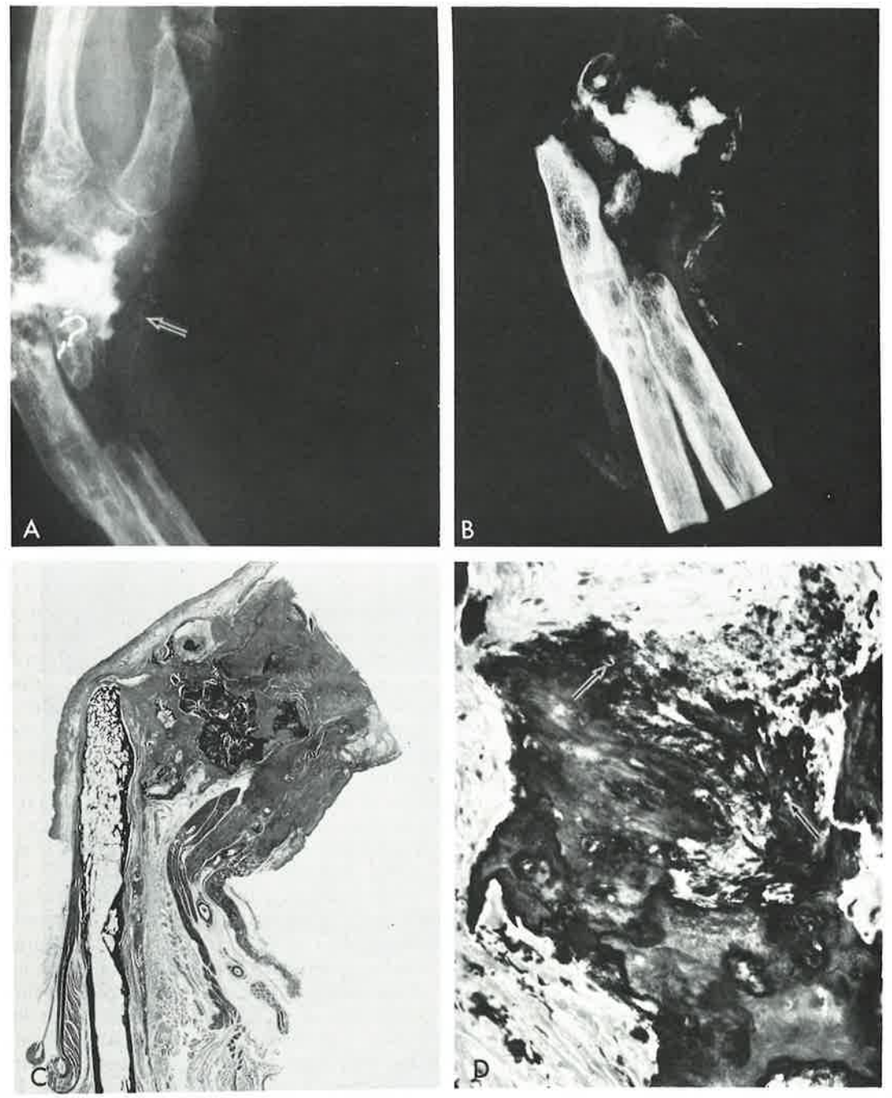

Figure 11. Solid, patchy density; radiation necrosis of the wrist. *A*, A clinical radiograph (lateral view) taken 55 years after radium implants and external radiotherapy of a recurrent giant cell tumor of the radius reveals an extensive area of patchy, solid, increased density coexisting with adjacent osteoporosis and contracture deformity. Palmar displacement of the mineralized radial artery (*arrow*) is a result of postradiation fibrosarcoma. *B*, The specimen radiograph demonstrates the patchy solid density in better detail. *C*, The correlating macrosection (magnification × 1) shows that the basophilic (black) area that corresponds to the patchy solid density is surrounded by postradiation fibrosarcoma (*dark gray*). *D*, A photomicrograph (magnification × 252) shows the gradation of stippled dystrophic (mineralization within hyalinized fibrous tissue into ischemic osteoid matrix.) There are few "osteocytic" cells (*arrows*). The combination of dystrophic mineralization and ischemic osteoid, both of which accept heavy mineralization, accounts for the solid, patchy, dense areas seen in the radiographs (*A* and *B*). The histologic findings are similar to the dystrophic mineralization and ischemic bone formation associated with bone infarcts and ossifying lipomas. (AFIP Neg. Nos. 78-5654-1, 81-14549, 81-14552, 81-14553.)

may cause sufficient trabecular bone destruction to be seen as lytic defects, but their indolent behavior allows time for bony reinforcement of adjacent, intact trabeculae. This results in coarsened trabeculae and a mottled radiographic pattern of combined lucency and increased density.

Reactive bone formation may be stimulated by inflammatory disorders, not only as a reinforcing margin (Part I, Fig. 10) or periosteal reaction, but also as internal endosteal and trabecular sclerosis, especially with chronic, low-grade osteitis and osteomyelitis. This can result in homogeneous areas of increased cloud-like density (Fig. 12, *A* and *B*) which, based on the radiographic density pattern alone, may be difficult to distinguish from osteosarcoma. A solid, ivory-like density pattern can also be seen in osteomyelitis. The infiltrating inflammatory process stimulates conversion of the marrow reserve into functional osteoblasts, with apposition of new layers of predominantly lamellar bone on pre-existing normal cancellous bone (Fig. 12*C*). Occasionally, abundant endosteal new bone formation can contribute to a homogeneous, ivory-like pattern of density under similar circumstances.

CARTILAGE MATRIX

Most of the embryonic skeleton is preformed in cartilage. A large volume of cartilage is subsequently created and removed during fetal and postnatal growth and development. Mineralization of anomalous, metaplastic, and neoplastic cartilage matrix is physiologically similar, if not identical to, the later stages of normal cartilage growth, maturation, and mineralization. Cartilage cell proliferation is followed by matrix secretion, hypertrophy and death of cartilage cells, provisional calcification of chondroid matrix, and then chondrolysis and replacement by enchondral bone.[1] However, the parallel stages of cartilage proliferation, maturation, provisional calcification, and enchondral bone replacement in cartilage tumors and tumor-like lesions are distorted by the lack of uniform maturation and the varied size of proliferating cartilage lobules. Under these circumstances, the normally orderly, linear, radiographically dense zone of provisional calcification and enchondral bone formation, seen at the physeal growth plate, is caricatured by a randomly distributed pattern of provisional calcification (stipples, which can coalesce and form floccules) and enchondral bone formation (rings and arcs) (Fig. 13).

The family of tumors and tumor-like lesions in which cartilage matrix is the main cell product has a wide variety of patterns and prognoses. The common benign lesions of the cartilage that are collectively known as chondromas (osteochondroma, cortical chondroma, and enchondroma) originate from the physeal growth plate as anomalies, rather than de novo neoplasms. These contrast with the more cellular, benign, proliferative lesions of cartilage, such as chondroblastoma and chondromyxoid fibroma, whose origins are less clear.

Chondrosarcomas may be primary or secondary.[4] In the authors' experience, the majority of chondrosarcomas that become malignant in the fourth, fifth, and sixth decade of life arise secondarily from pre-existing benign chondromas. The less common primary chondrosarcomas that develop during adolescence or young adulthood frequently involve the metaphyses of long bones and the axial skeleton, especially the pelvis. The reported rarity of chondrosarcoma in the developing skeleton, as well as the high-grade variants may, in large part, relate to adherence to the criterion that any amount of tumor bone warrants classification as osteosarcoma. Like their osseous counterparts, parosteal chondrosarcomas arise on the surface of the bone. Histologic recognition of malignant processes, as with other tumors, is based upon an excessive variation in the size, shape, and staining characteristics of cells beyond the range of normal (see Fig. 19*E*). In general, primary, intraosseous chondrosarcomas tend to act as high-grade malignant lesions, parosteal chondrosarcomas as low-grade malignant lesions, and secondary chondrosarcomas[10, 22] generally range from low-grade, well-differentiated chondrosarcomas (see Fig. 19) to undifferentiated sarcomas with a dominant spindle cell pattern (see Fig. 20).

Mineralization Patterns of Tumor Cartilage

The stippled mineralization pattern of tumor cartilage matrix is most commonly seen in enchondromas (Fig. 14, *A, B,* and *D*) and osteochondromas (see Fig. 17, *A* and *C*). Correlation of a specimen radiograph (Fig. 14*B*) and histologic sections (Figs. 14*D* and

Text continued on page 806

Figure 12. Cloud-like density; sclerosing osteomyelitis of the tibia. *A*, The clinical radiograph shows a diffuse, hazy to cloud-like, increased density of the proximal tibial metaphysis and upper diaphysis which is associated with a solid, wide, periosteal reaction. *B*, A clinical radiograph taken eight months later reveals an increase in the cloud-like density pattern, reminiscent of that seen with sclerosing osteosarcoma. The periosteal fill-in and incorporation and the lack of progression (no bone destruction or soft tissue extension) over the eight months support the diagnosis of a benign process. *C*, A photomicrograph (magnification × 63) shows appositional thickening of cancellous bone by new layers of lamellar bone being formed by active osteoblasts. The intervening marrow has undergone fibrovascular conversion and is populated by chronic inflammatory cells. The thickening and reinforcement of the pre-existing bony trabeculae, along with endosteal and periosteal new bone formation, results in the diffuse, hazy increased, cloud-like density seen in the clinical radiograph (*A* and *B*). (AFIP Neg. Nos. 70-11100-13, 70-11100-6, 81-16758.)

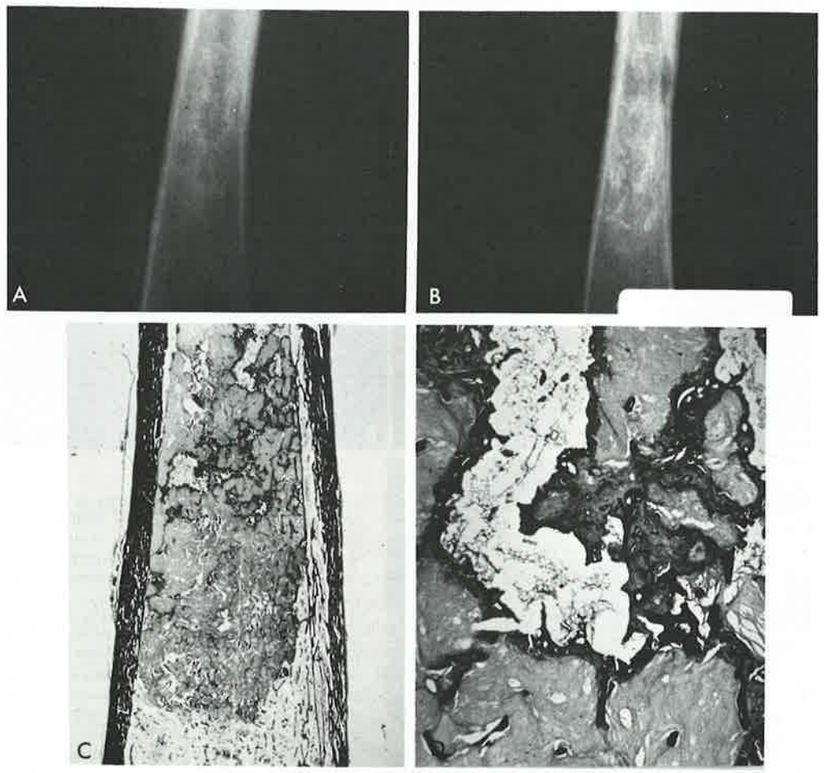

Figure 13. Rings and arcs; enchondromas of the femur. *A*, A clinical radiograph reveals a ring and arc pattern with occasional stipples and rare floccules within the medullary cavity, as well as a periosteal reaction. This endosteal ring and arc pattern of mineralization is typically seen with chondromas. *B*, A specimen radiograph better delineates the ring and arc pattern and the stipples associated with endosteal scalloping. *C* and *D*, A macrosection (magnification × 1) and a photomicrograph (magnification × 15) show the intramedullary lobules of proliferating cartilage, partially encircled by rings and arcs of enchondral bone which account for the ring and arc densities on the radiographs. (AFIP Neg. Nos. 72-12889-1,2, 81-16760, 81-14786.)

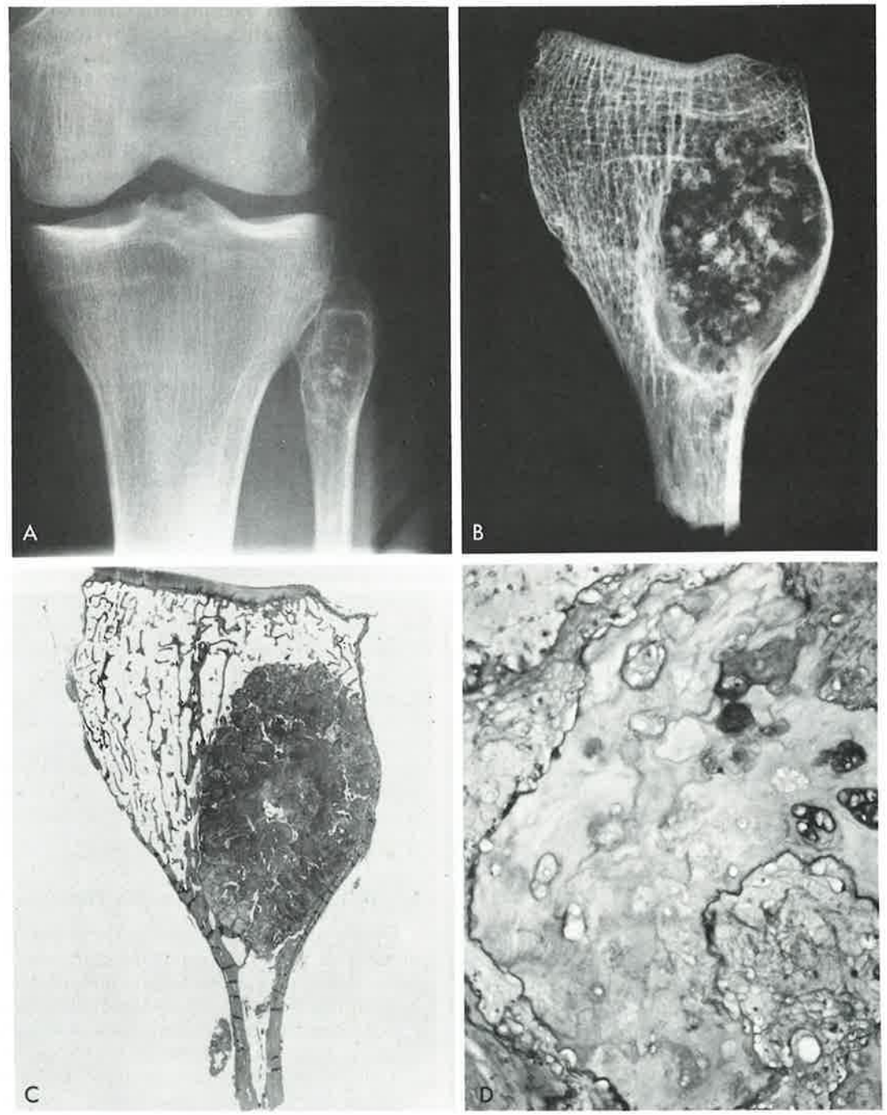

Figure 14. Stippled to flocculent density; enchondroma of the fibula. *A*, A clinical radiograph of the knee shows that the proximal fibula contains a lucent defect with widened bone contour and a well-defined, slightly reinforced margin. An internal stippled to flocculent density pattern is seen. *B*, A specimen radiograph (magnification × 2) demonstrates the stipples and floccules in much better detail. Some of the floccules have slightly irregular to finely stippled margins. The presence of faint rings and arcs can also be appreciated in this proliferating cartilage lesion, characterized by lobular growth. The widened contour (shell) and reinforced margin (sclerotic edge) are reassuring features of slow growth. *C* and *D*, A macrosection (magnification × 1) and a photomicrograph (magnification × 157) demonstrate the hyaline cartilage pattern of enchondroma. The range of stain intensity in the photomicrograph correlates with the variable degrees of cartilage mineralization. These areas are analagous to provisional zones of calcification in growth plate cartilage and account for the stippled and flocculent pattern in the clinical radiograph. (AFIP Neg. Nos. 79-6002, 81-14569, 81-14594, 81-14515.)

17*C*) indicates that the stipples reflect small foci of heavily mineralized hyaline cartilage matrix. Mineralization in the more mature hyaline matrix component of chondromas reemphasizes its analogous relationship to the zone of provisional "calcification" in normal maturing cartilage at the growth plate.

The stippled pattern of cartilage matrix mineralization can occasionally be seen in otherwise typically lucent chondroblastomas (Fig. 15). Histologically, mineralization in chondroblastomas can be subdivided. The thin network of chondroid matrix elaborated by individual tumor cells may become mineralized (see Fig. 15*B*). Rarely is this matrix of sufficient quantity to contribute significantly to increased radiographic density. The other pattern of mineralization occurs in the collagen-rich, chondroid, matrix islands as a compact crystalline aggregate (Fig. 15, *B* and *C*). These diffusely scattered mineral deposits can create a finely stippled pattern of increased density that is evident on radiography (Fig. 15*A*).

In general, as the hyaline cartilage matrix of chondromas continues to mature and become mineralized, the enlargement and confluences of stipples creates floccules (Fig. 16). An admixture of stipples and floccules is seen with considerable frequency in both benign (see Fig. 14) and malignant (see Fig. 18) cartilage lesions.[24] In these cartilage lesions, the flocculent pattern is readily recognized in clinical (Figs. 14*A* and 18*A*) and specimen radiographs (Fig. 14*B*). Histologic sections (Figs. 14, *C* and *D*; 15, *B* and *C*; and 16, *B* and *C*) indicate that stippled and flocculent density patterns represent heavily mineralized hyaline cartilage matrix.

The final stage of cartilage cell death and removal is followed by enchondral bone formation. Because chondromas grow as variously sized lobules of proliferating cartilage cells, the enchondral bone takes the form of radiographically recognizable rings and arcs. Again, both benign cartilage lesions, such as enchondromas (see Fig. 13) and focally malignant cartilage lesions (see Fig. 19), will frequently demonstrate rings and arcs.

The concurrence of enchondral bone rims (rings and arcs) with focally mineralized cartilage matrix (stipples and floccules) occurs with considerable frequency (Figs. 13, 14, 16, and 19). Some observers combine these component mineralization patterns when explaining the "flocculent" radiographic pattern of cartilage lesions.[18, 19] We believe that the two patterns warrant separate recognition since these densities originate from a different process; either can dominate in individual cases (compare Figs. 16 and 19) or occur separately.

Marked, ill-defined patches of solid density can occasionally be seen in cartilage lesions, especially in the base of osteochondromas (Fig. 17). This is predominantly attributable to highly mineralized, hypocellular, chondroid matrix that remains in the base during growth of the lesion (Fig. 17*C*); some enchondral bone; and, to a lesser extent, ischemic-appearing, mineralized, fibrofatty marrow (Fig. 17*B*).

Radiographic signs of cartilage matrix mineralization and induction of enchondral bone formation denote mature cartilage matrix, but do not necessarily preclude coexistent malignant areas (Fig. 19), even of relatively high grade (Fig. 20). This is because histologic grade is not necessarily uniform throughout a lesion (Fig. 19). The long-recognized correlation of loose, textured matrix with more aggressive cartilage lesions[2] has recently been reaffirmed by sophisticated biochemical analyses. These analyses established water content as a prognostically significant variable.[21] However, malignant cartilage (Fig. 18, *B* and *C*) can exhibit a definite mineralized hyaline character. Correlation of clinical behavior with the multiple and varied radiographic patterns that chondroid lesions exhibit, such as margins, periosteal reactions, and mineralized matrix, may help to clarify the current prognostic uncertainties.

Dystrophic Mineralization Patterns

Dystrophic mineralization is the deposition of mineral salts within degenerating and necrotic tissue, primarily necrotic fat and densely hyalinized connective tissue. Within bone, this process can result in stippled, flocculent, solid, patchy, and linear density patterns. Histologically, dystrophic mineralization initially appears as finely distributed basophilic granules within a hypocellular, degenerating tissue background that serves as a matrix (see Fig. 10*B*).

The accumulation of dystrophic mineralization in injured and necrotic fat may be accompanied by the formation of a peculiar, coarse, fiber bone, or "ischemic bone" (see Fig. 10*C*). The coalescence of dystrophic mineralization and superimposition of ischemic bone (Fig. 10*D*) accounts for the patchy,

Text continued on page 811

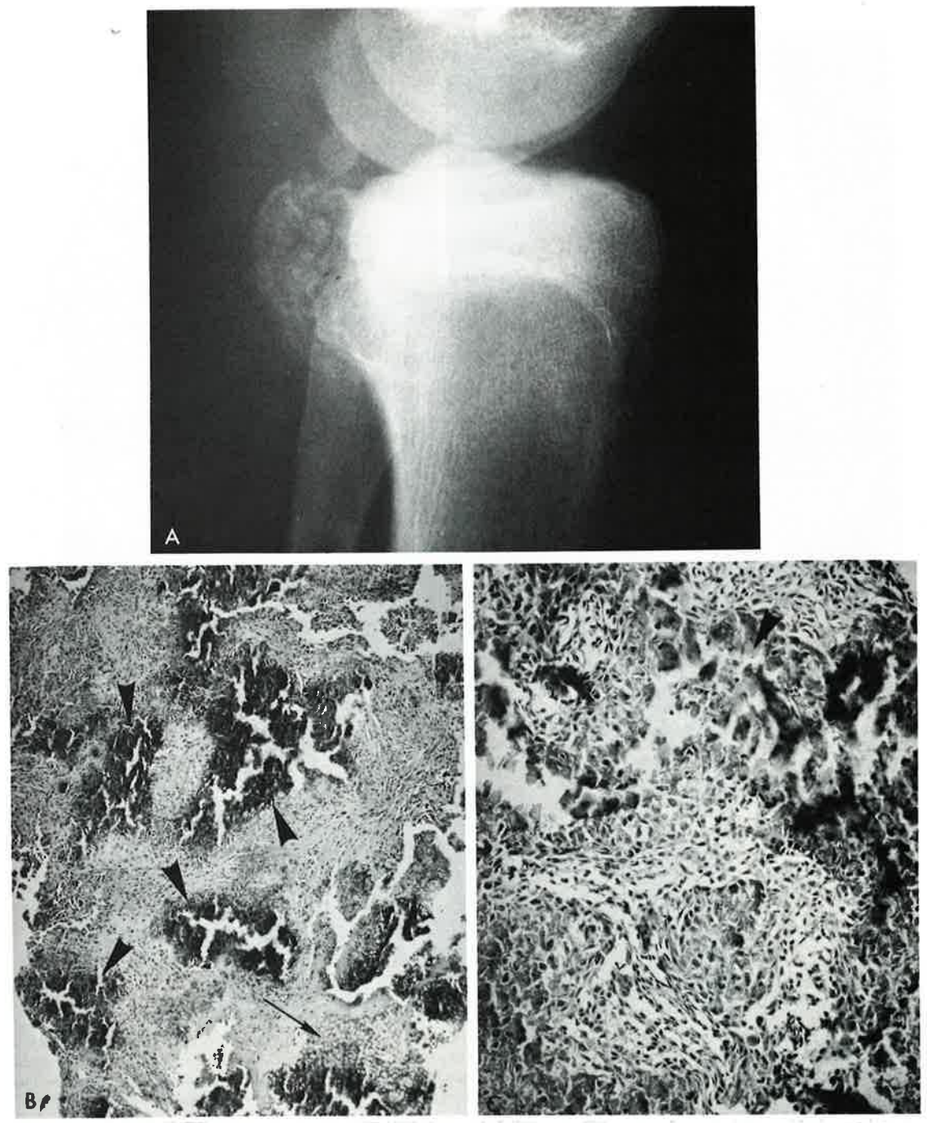

Figure 15. Stipples: chondroblastoma of the tibia. *A*, A lateral clinical radiograph shows a lesion causing a widening of the contour of the posteromedial aspect of the proximal tibial epiphysis. The faint stippled pattern of increased density is present throughout the lesion. *B*, A photomicrograph (magnification × 63) shows matrix elaboration about the individual chondroblastic cells (*arrow*) and numerous foci of matrix mineralization (*arrowheads*). *C*, A photomicrograph (magnification × 157) more clearly demonstrates the chondroblastic pattern with its matrix distribution about the individual tumor cells, foci of mineralization, and areas of degenerating tumor cells (*arrowhead*). Although there is mineralization of collagenous chondroid matrix about the individual chondroblastic cells, the increased mineralization within the hypocellular chondroid primarily accounts for the finely stippled densities seen in the clinical radiograph. (AFIP Neg. Nos. 81-2506, 81-16754, 81-16753.)

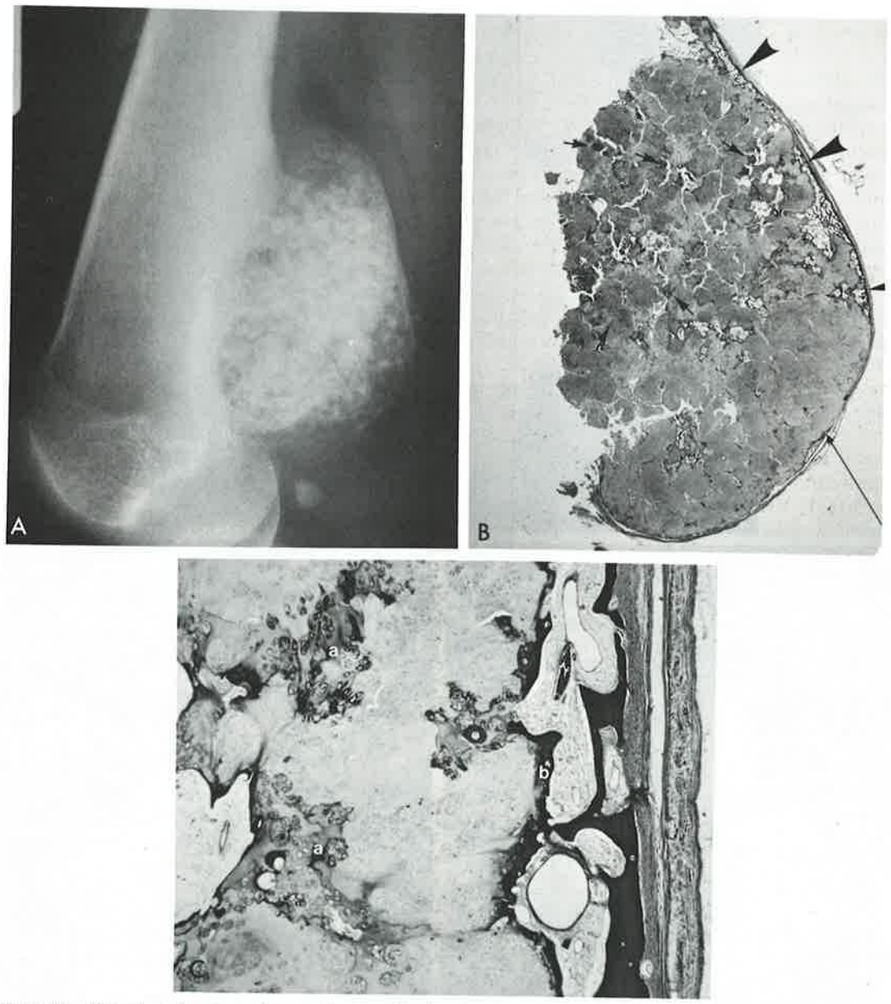

Figure 16. Flocculent density; active, sessile osteochondroma of the femur. *A*, A clinical radiograph demonstrates a "sessile" osteochondroma arising from the posterior distal femur, the features of which are reminiscent of a parosteal tumor. The bony stalk is partially obscured by the predominantly flocculent densities and occasional rings and arcs. The outer perimeter is defined in part by a bony plate. *B*, The macrosection (magnification × 2) depicts the lobular growth pattern of cartilage tumors. The irregular, dark-staining patches (*arrows*) within the pale-staining cartilage correlate with the flocculent densities in the clinical radiograph. A partial bony shell (*arrowheads*) forms after reduced proliferative capacity of the cartilage cap results in its loss through enchondral ossification. Other areas of the cartilage cap persist with a perichondrium (*long arrow*). *C*, A photomicrograph (magnification × 25) demonstrates areas of mineralized cartilage matrix (a) and enchondral bone formation (b) partially outlining the cartilage lobules. These areas account for the combined flocculent and ring and arc density patterns, respectively. The partial bony shell is well formed (*right side*). (AFIP Neg. Nos. 76-2618-1, 81-14521, 81-14523.)

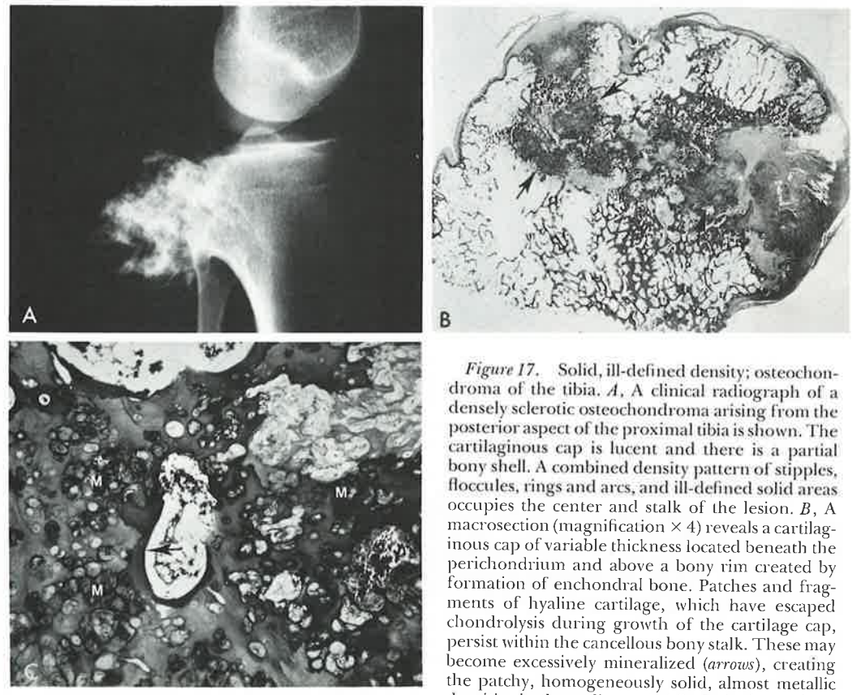

Figure 17. Solid, ill-defined density; osteochondroma of the tibia. *A*, A clinical radiograph of a densely sclerotic osteochondroma arising from the posterior aspect of the proximal tibia is shown. The cartilaginous cap is lucent and there is a partial bony shell. A combined density pattern of stipples, floccules, rings and arcs, and ill-defined solid areas occupies the center and stalk of the lesion. *B*, A macrosection (magnification × 4) reveals a cartilaginous cap of variable thickness located beneath the perichondrium and above a bony rim created by formation of enchondral bone. Patches and fragments of hyaline cartilage, which have escaped chondrolysis during growth of the cartilage cap, persist within the cancellous bony stalk. These may become excessively mineralized (*arrows*), creating the patchy, homogeneously solid, almost metallic densities in the radiograph (*A*). *C*, A photomicrograph (magnification × 63) of the darkly stained, anachronistic stalk shows cartilage where dense mineralization has occurred (m). Enchondral bone is also applied to cartilage (*arrow*). (AFIP Neg. No. 77-307-3, 81-14528, 81-14530.)

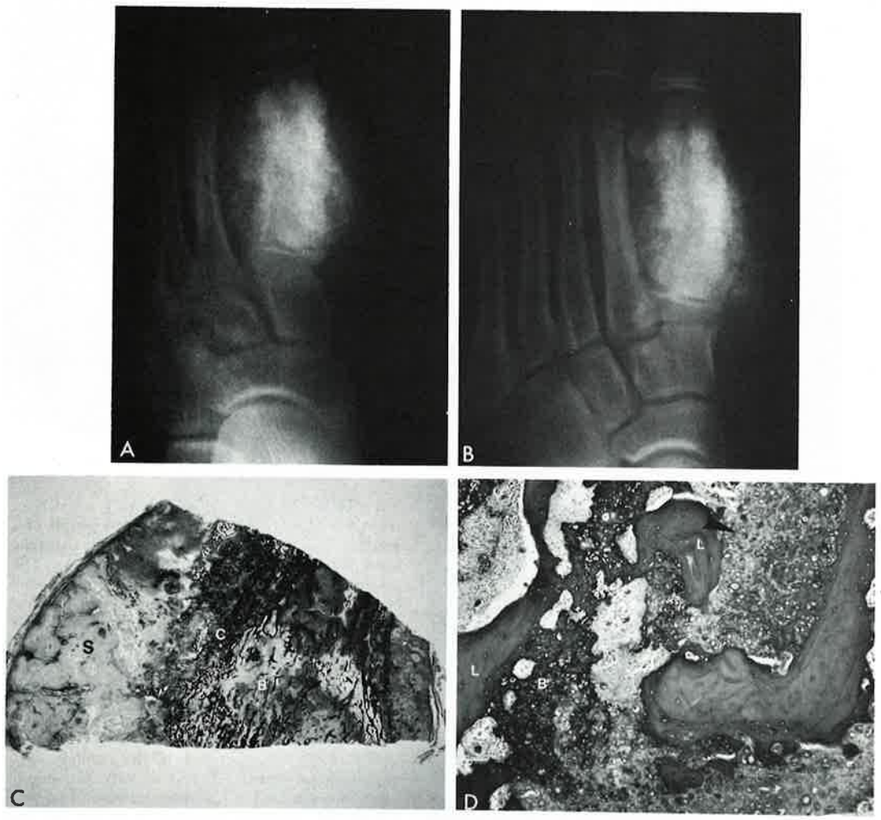

Figure 18. Flocculent density; primary chondrosarcoma of the first metatarsal bone. *A* and *B*, Clinical radiographs (anteroposterior and oblique views, respectively) show flocculent densities with some stipples associated with cortical destruction and tumor extension into soft tissue. The adjacent metatarsal bone shows cortical thickening and a periosteal reaction. The growth plate of the proximal first metatarsal bone has prevented tumor extension into the epiphysis. *C*, A transverse section (magnification × 2.3) of the metatarsal bone indicates that the extensive sarcoma filling the medullary space (B) with cortical destruction (C) and soft tissue extension (S) is predominantly cartilaginous. *D*, A photomicrograph (magnification × 63) shows that the sarcomatous matrix which abuts the pre-existent lamellar bone (L) has osseous (B) and cartilaginous (*arrowhead*) characteristics. The two matrices grade into each other, forming a gradual continuum. The areas of darker staining correlate with greater mineralization and account for the flocculent density pattern in the clinical radiograph (*A* and *B*). (AFIP Neg. Nos. 75-10167-1,2, 81-14524, 81-14526.)

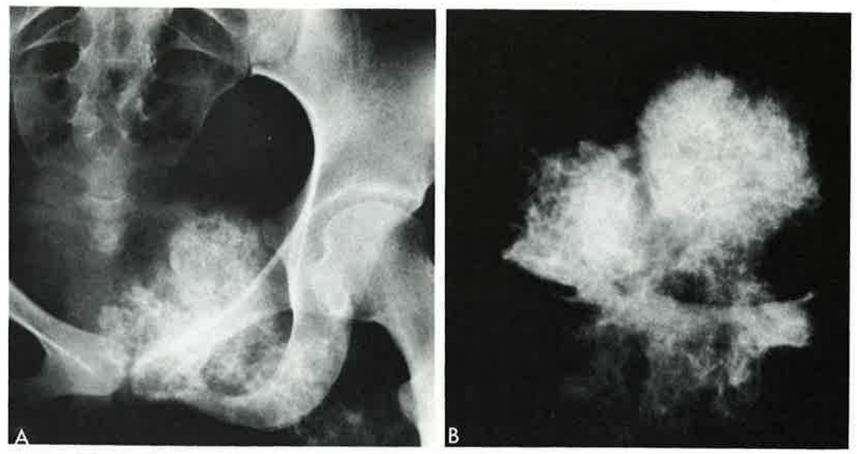

Figure 19. Stipples, floccules, rings and arcs; low-grade, secondary chondrosarcoma arising in an osteochondroma affecting the pubis. *A*, A clinical radiograph shows a tumor arising from the pubic bone. Its ring and arc pattern predominates over the stippled and flocculent density patterns. *B*, A specimen radiograph (magnification × 1) depicts the ring and arc pattern in greater detail.

Illustration continued on following page

sclerotic areas of radiographic density in intraosseous lipomas (see Fig. 10*A*). The fat within the center of the lipomas is at the highest risk for ischemic degeneration and ossification. For this reason, the marked mineral densities of ossifying lipomas are usually found within the lesion rather than around the perimeter (see Fig. 10*A*).

In contrast to ossifying lipomas, bone infarcts are nonproliferative lesions resulting from ischemic necrosis of marrow fat and cancellous bone. Under these circumstances, the repair process begins at the peripheral margin of the lesion. The inner zone of the perimeter is composed primarily of necrotic fat which may undergo dystrophic mineralization (see Fig. 9*E*). The reactive process creates an encapsulating, outer, fibrous margin which, because of relative ischemia, becomes partially hyalinized and also incurs dystrophic mineralization. The combination of ischemic bone and dystrophic mineralization around the infarct's circumference results in the linear whisps, curls, and "rising smoke" density patterns seen at the perimeter of the typical bone infarct (see Fig. 10, *A* through *C*).[28] Another distinguishing feature of ossifying lipomas is the absence of features indicating proliferative enlargement, such as rounded sclerotic rims of uniform width or widened bone contours.

Dystrophic mineralization within densely hyalinized connective tissue and injured marrow resulting from radiation necrosis (see Fig. 11*D*) may also result in similar dense patches of mineralization (Fig. 11, *A* through *C*).

Mineralization can also be seen within soft tissue lesions, especially those in and about joints of long bones. Examples include synovial chondromatosis, calcific bursitis, and tumoral calcinosis.[20]

SUMMARY

The mineralized matrix patterns demonstrated in clinical radiographs of primary bone neoplasms and related disorders help to predict matrices, and have diagnostic significance. These radiographic patterns may yield important clues as to the true nature of a lesion, especially when only limited biopsy material is available from extraosseous or nonrepresentative areas. Therefore, in the evaluation of bone tumors and tumor-like conditions, it is of extreme importance to correlate the histologic findings with the radiographic examination and to know precisely the location at which the biopsy material was obtained.

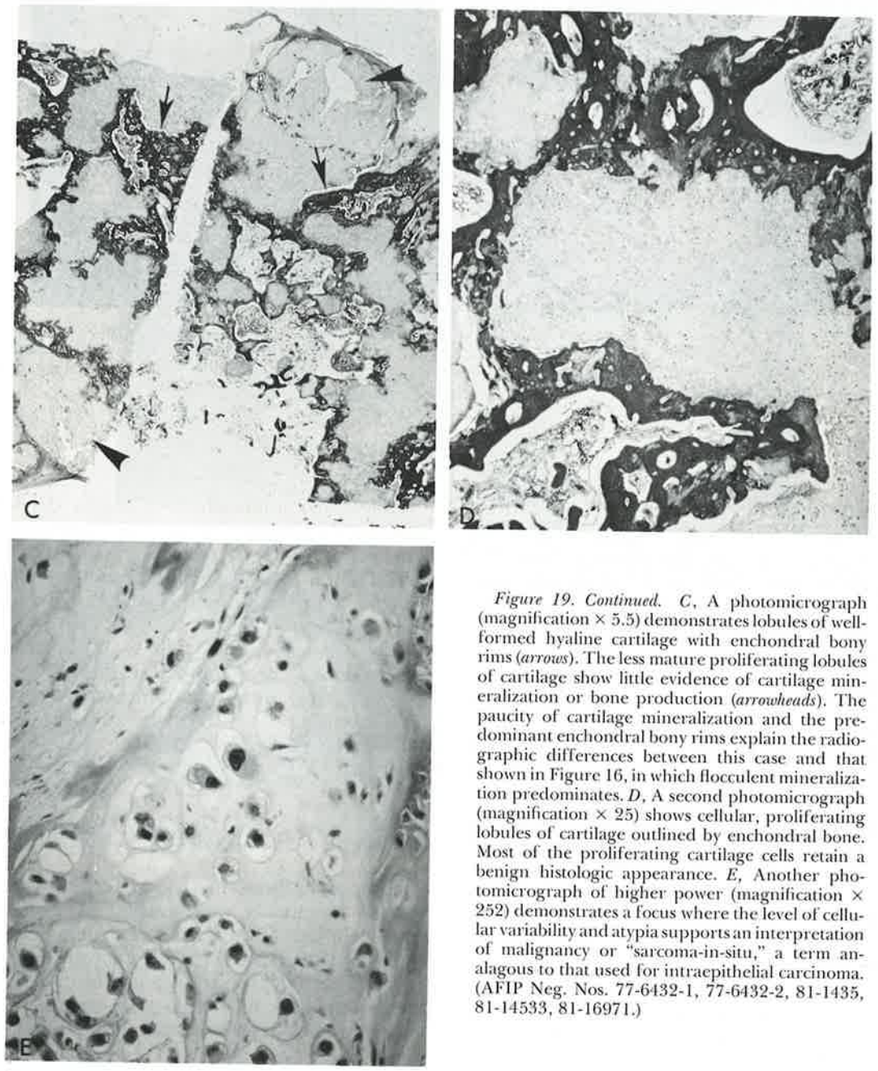

Figure 19. Continued. *C*, A photomicrograph (magnification × 5.5) demonstrates lobules of well-formed hyaline cartilage with enchondral bony rims (*arrows*). The less mature proliferating lobules of cartilage show little evidence of cartilage mineralization or bone production (*arrowheads*). The paucity of cartilage mineralization and the predominant enchondral bony rims explain the radiographic differences between this case and that shown in Figure 16, in which flocculent mineralization predominates. *D*, A second photomicrograph (magnification × 25) shows cellular, proliferating lobules of cartilage outlined by enchondral bone. Most of the proliferating cartilage cells retain a benign histologic appearance. *E*, Another photomicrograph of higher power (magnification × 252) demonstrates a focus where the level of cellular variability and atypia supports an interpretation of malignancy or "sarcoma-in-situ," a term analagous to that used for intraepithelial carcinoma. (AFIP Neg. Nos. 77-6432-1, 77-6432-2, 81-1435, 81-14533, 81-16971.)

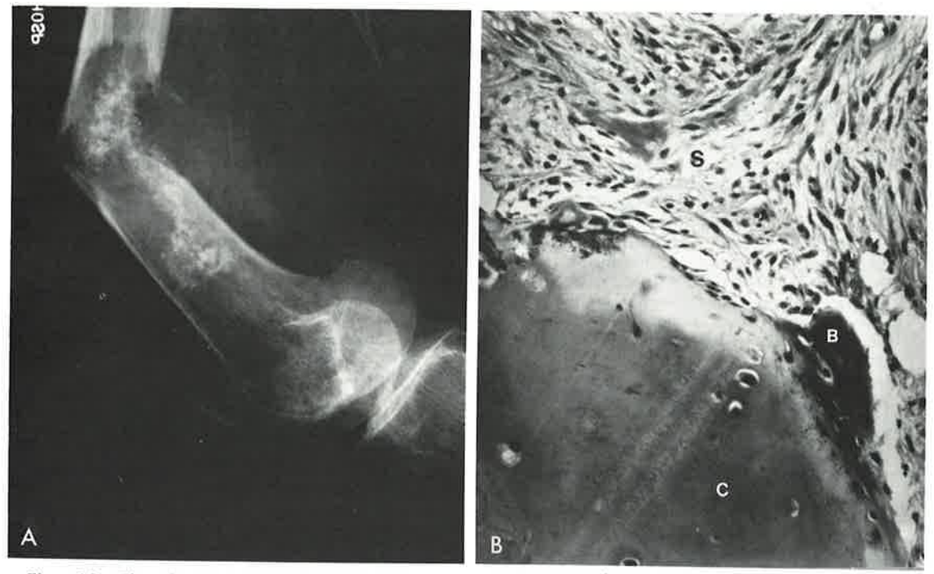

Figure 20. Flocculent and ring and arc density patterns with osteolysis and pathologic fracture; enchondroma with high-grade sarcomatous change affecting the femur. *A*, A clinical radiograph confirms the presence of a long-standing lesion of the cartilage as evidenced by the flocculent and ring and arc density patterns within the medullary cavity. The superimposed osteolysis and pathologic fracture are ominous, aggressive features. *B*, A photomicrograph (magnification × 252) reveals benign hyaline cartilage (C) separated from spindle cell sarcoma (S) by a rim of ossification (B). Benign-to-malignant transitions of this type can be misinterpreted as "dedifferentiated chondrosarcoma." (AFIP Neg. Nos. 73-2619, 81-17011.)

Patterns of mineralization may be the only remnants of a pre-existing lesion that has undergone sarcomatous transformation, such as in bone infarcts, enchondromas, or osteochondromas. The pre-eminent item of importance for patient care is the diagnosis of a malignant process. However, failure to appreciate antecedent benign conditions will not contribute toward a better understanding of tumor biology or a determination of those benign lesions that warrant removal or close clinical follow-up.

Integration of matrix data with knowledge of the anatomic location of a lesion, the character of its margins, and the periosteal reaction patterns it produces permits prognostication and often, specific diagnosis.

ACKNOWLEDGMENT

We thank the many contributing radiologists and pathologists whose case material illustrated this work, as well as the Armed Forces Institute of Pathology's secretarial and technical staff from the Departments of Radiologic Pathology, Orthopedic Pathology, and Medical Illustration, for their assistance.

REFERENCES

1. Bloom, W. F., and Fawcett, D. W.: Bone. *In* A Textbook of Histology. Ch. 7. Philadelphia, W. B. Saunders Co., 1962, pg. 164.
2. Codman, E. A.: The nomenclature used by the Registry of Bone Sarcoma. Am. J. Roentgenol., *13*:105–126, 1925.
3. Codman, E. A.: Registry of Bone Sarcoma. Part I. Twenty-five criteria for establishing the diagnosis of osteogenic sarcoma. Part II. Thirteen registered cases of "five year cures" analyzed according to these criteria. Surg. Gynecol. Obstet., *42*:381–393, 1926.
4. Dahlin, D. C.: Chondrosarcoma (primary, secondary, dedifferentiated, and clear cell). *In* Bone Tumors: General Aspects and Data on 6221 Cases. Ed. 3. Ch. 17. Springfield, Illinois, Charles C Thomas Co., 1978, pp. 190–217.
5. Dahlin, D. C., and Unni, K. K.: Osteosarcoma of bone and its important recognizable varieties. Am. J. Surg. Pathol., *1*:61–72, 1977.
6. Ewing, J.: The classification and treatment of bone

sarcoma. *In* Report of the International Conference on Cancer. Bristol, John Wright and Sons, 1928, pp. 365–376.
7. Gschnitzer, F., and de Gennars, P. F.: Das osteoid osteoma. Klinik, Pathomorphologie und gedanken zur ätiologie. z. Orthop., *86*:1–14, 1955.
8. Hall, B. K.: Cellular differentiation in skeletal tissues. Biol. Rev., *45*:455–484, 1970.
9. Huntington, R. W., and Huntington, R. W., III: Classification of neoplasms: A critical appraisal. Perspect. Biol. Med., Winter, 1977, pp. 215–222.
10. Huvos, A. G.: Cartilage-forming tumors — malignant. *In* Bone Tumors: Diagnosis, Treatment, and Prognosis. Ch. 13 and 14. Philadelphia, W. B. Saunders Co., 1979, pp. 206–242.
11. Illustrated Tumor Nomenclature. The International Union Against Cancer, Committee on Tumor Nomenclature. New York, Springer-Verlag, p. 258, 1965.
12. International Classification of Diseases. Vol. 1. World Health Organization. 1975 (revision), p. 682.
13. Jaffe, H. L.: Benign osteoblastoma. Bull. Hosp. Joint Dis., *17*:141–151, 1956.
14. Jaffe, H. L.: Tumors and Tumorous Conditions of the Bones and Joints. Philadelphia, Lea and Febiger, 1958.
15. Johnson, L. C.: A general theory of bone tumors. Bull. N. Y. Acad. Med., *29*:164–171, 1953.
16. Johnson, L. C.: The kinetics of skeletal remodeling in structural organization of the skeleton. Birth Defect Original Article Series. Vol. 2. National Foundation of March of Dimes, April, 1966.
17. Johnson, L. C.: Morphologic analysis in pathology. The kinetics of disease and general biology of bone. *In* Frost, H. M. (ed.): Bone Biodynamics. Ch. 29. Boston, Little, Brown and Company, 1964, pp. 543–654.
18. Lodwick, G. S.: The bone and joints. *In* Atlas of Tumor Radiology. Chicago, Year Book Medical Publishers, Inc., 1971.
19. Lodwick, G. S.: A systemic approach to roentgen diagnosis of bone tumors. *In* M. D. Anderson Hospital and Tumor Institute: Tumors of Bone and Soft Tissue. Chicago, Yearbook Medical Publishers, Inc., 1965, pp. 49–68.
20. Madewell, J. E., and Sweet, D. E.: Tumor and tumor-like conditions in or about joints. *In* Resnick, D., and Niwayama, G. (eds.): Diagnosis of Bone and Joint Disorders. Vol. 3. Ch. 74. Philadelphia, W. B. Saunders Co., 1981.
21. Mankin, H. J., Cantley, K. P., Lippiello, L., et al.: The biology of human chondrosarcoma. I. Description of the cases, grading, and biochemical analyses. J. Bone Joint Surg., *62A*:160–176, 1980.
22. Mirra, J. M.: Intraosseous cartilage and chondroid-producing tumors. *In* Bone Tumors: Diagnosis and Treatment. Philadelphia, J. B. Lippincott Co., 1980, pp. 162–256.
23. O'Hara, J. P., Tegtemeyer, C., Sweet, D. C., et al.: Angiography in the diagnosis of osteoid osteoma of the hand. J. Bone Joint Surg., *57A*:163–166, 1975.
24. Phemister, D. B.: Chondrosarcoma of bone. Surg. Gynecol. Obstet., *50*:216–233, 1930.
25. Phemister, D. B.: A study of the ossification in bone sarcoma. Radiology, *7*:17–23, 1926.
26. Spjut, H. J., Dorfman, H. D., Fechner, R. E., and Ackerman, L. U.: Tumors of bone and cartilage. *In* Atlas of Tumor Pathology. Series 2. No. 5. Washington, D. C., Armed Forces Institute of Pathology, 1971.
27. Standard Nomenclature of Diseases and Operations. Ed. 5. American Medical Association. New York, McGraw-Hill Book Co., 1961, p. 97.
28. Sweet, D. E., and Madewell, J. E.: Pathogenesis of osteonecrosis. *In* Resnick, D., and Niwayama, G. (eds.): Diagnosis of Bone and Joint Disorders. Vol. 3. Ch. 76. Philadelphia, W. B. Saunders Co., 1981.
29. Sweet, D. E., et al.: Unpublished data.
30. Systematized Nomenclature of Pathology (SNOP). Committee on Nomenclature and Classification of Disease. College of American Pathologists. Ed. 1. 1965, p. 121.
31. Unni, K. K., Dahlin, D. C., McLeod, R. A., et al.: Intraosseous well-differentiated osteosarcoma. Cancer, *40*:1337–1347, 1977.
32. Van der Heul, R. O., and Von Ronnen, J. R.: Parosteal osteosarcoma. Differential diagnosis, treatment, and an analysis of 80 cases. J. Bone Joint Surg., *49A*:415–439, 1967.

Department of Orthopedic Pathology
Armed Forces Institute of Pathology
Washington, D.C. 20306

Cumulative Index, 1979–1981

Note: Page numbers of symposium and article titles are in **boldface** type.